J Therm Anal Calorim (2012) 108:985–989
DOI 10.1007/s10973-011-1981-z

Studies of physico-chemical properties and fractal dimensions of MgB_2 superconductor surface

G. W. Chądzyński · P. Staszczuk · D. Sternik · M. Błachnio

ICVMTT2011 Conference Special Chapter

Abstract The porous structure of MgB_2 has been investigated using atomic force microscopy (AFM) and sorption techniques. The fractal dimension and surface roughness parameters were evaluated from (AFM) and nitrogen adsorption–desorption isotherms measured at −196 °C for MgB_2 sample. Adsorption capacity, specific surface area, and fractal dimensions were determined from adsorption–desorption isotherms. The sorption isotherms of MgB_2 samples were S-shaped and belong to type II according to the IUPAC classification. The results of fractal dimensions of MgB_2 surface determined on the basis sorptometry and AFM data are compared.

Keywords Atomic force microscopy (AFM) · Sorptometry methods · Fractal dimensions · Surface roughness parameters of MgB_2

Introduction

The discovery of superconductivity at −234 °C in magnesium diboride, MgB_2 [1] has attracted much interest in and research on this material because of the apparent simplicity of its chemical composition, crystal structure, and electronic properties. MgB_2 belong to a very simple hexagonal structure (AlB_2-type, space group *P*6/mmm) comprising graphitic type B layers interleaved with Mg layers. It has the highest critical temperature, which is far from liquid helium temperature (−269 °C), among all of the known binary intermetallic superconductors. Comparing with the high-T_c oxide superconductors, it possesses a larger coherence length of 3–12 nm, current density even in high magnetic field. These properties convince scientists that MgB_2 will be very powerful material, to replace, up to now used superconducting NbTi and Nb_3Sn. Since the discovery of superconductivity in MgB_2 researchers have made much effort to synthesize high quality samples of MgB_2. The polycrystalline bulk MgB_2 is obtained by direct reaction of the elements in inert gases atmosphere (Ar, He, and N_2) or under vacuum [2, 3]. Different synthesis methods have been applied by the researchers to prepare dense MgB_2 bulk samples. One is *ex-situ* "powder in tube" technique involves direct filling metallic tubes with commercial MgB_2 powder and then drawing and rolling into tapes followed by sintering at relative high temperatures (800–1000 °C) [4, 5]. An alternative approach (in situ "powder in tube" technique) is characterized by filling the metallic tubes with elemental Mg and B powders and subsequent drawing and rolling into tapes followed by heat treatment, during which the elements react to form MgB_2. This reaction can be performed at lower temperatures (600–700 °C) than that required sintering of MgB_2. This is beneficial to circumvent or reduce undesirable reactions of Mg and B with the sheath material [6]. Another synthesis method is use MgH_2 powder instead of Mg [7–9].

The third approach of the "powder in tube" process is characterized by the use of partially reacted precursor [10,

G. W. Chądzyński (✉)
Technical–Economic Faculty, Humanity College, Stabłowicka Str. 95, 54-062 Wrocław, Poland
e-mail: g.chadzynski@o2.pl

P. Staszczuk
Faculty of Mathematics and Natural Sciences, Institute of Biotechnology, The John Paul II Catholic University of Lublin, Konstantynów 1H Str., 20-708 Lublin, Poland

D. Sternik · M. Błachnio
Department of Physicochemistry of Solid Surface, Chemistry Faculty, Maria Curie-Skłodowska University, M. Curie-Skłodowska Sq. 3, 20-031 Lublin, Poland

11]. Partial reaction of Mg with B is induced by mechanical alloying of Mg + B powder mixtures resulting in a precursor powder, consisting of reactive mixture Mg, B, and MgB_2. For this highly reactive powder, annealing temperatures 550–600 °C are sufficient to synthesize tapes.

Other processing methods include liquid magnesium infiltration technique of boron preforms [12], microwave synthesis [13].

There have been many investigations to establish the optimum synthesis conditions, doping C [14–20], Zr [21], Au [22], Al [23], Pb [24], La [25] as well as most suitable stoichiometry of Mg and B [26]. MgB_2 has been considered to have strong inter-grain connectivity, owing to its long coherence length. Porous microstructure, large scale defects such as cracks and impurity phases at grain boundaries are all candidates for current limiting factors in polycrystalline MgB_2. In a recent decade Williamson–Hall [27] or Rietveld analysis has been becoming a popular method to detect the grain size and micro strain of MgB_2 [28–32]. However, there are few studies discussing statistical mean of crystalline size analyzed from X-ray diffraction (XRD) data [33]. It has been suggested that grain boundaries in polycrystalline MgB_2 act as weak links. It is responsible for large microwave residual surface resistance R_s at low temperatures, and is source of nonlinearity [34, 35].

In this article, we report properties relating to porosity of solids (fractal dimensions, surface roughness parameters) evaluated from atomic force microscopy (AFM) and nitrogen adsorption–desorption isotherms measured at −196 °C for MgB_2 sample. Adsorption capacity, specific surface area, and fractal dimensions were determined from adsorption–desorption isotherms. The results of fractal dimensions of superconductor surface determined on the basis sorptometry and AFM data are compared.

Experimental

In situ bulk sample MgB_2 was fabricated by the "powder in closed tube" method. Mg powder (Merck, purity 99%, size ~ 40 μm) and B (Merck, purity 99.9%, size ~ 0.25 μm) were used as starting materials. Nb tubes filled by powder mixture Mg and B with a molar ratio of 1:2 were uniaxially pressed into a short tape shape with several centimeters in length and their both ends were closed by uniaxial pressing. Sample was heated at 800 °C for 6 h in an evacuated quartz ampoule, and then followed by quenching to room temperature. Single core conductors were deformed by swaging, drawing, and rolling after removing the sheath. Tapes with cross-section dimension of 4.0 × 0.3 mm were milled in ball mill (Retsch) to obtain a finer granulometry. The phase analysis was carried out by XRD using in a STOE diffractometer and Cu Kα radiation. The lattice parameters were determined from the *d*-values of the XRD peaks by a standard least-squares refinement method. The morphology of the sample was investigated using AFM (NanoScope III type, Digital Instruments, USA). Particle size distribution varying from 10 to 2000 nm. Nitrogen adsorption–desorption measurements at −196 °C were carried out using an automatic ASAP 2405V 1.01 volumetric adsorption analyzer (Micrometrics Instrument Corp, Norcross, GA, USA). The adsorption and porosity properties of the powder sample, as calculated from the adsorption measurements, are listed in Table 1. Before the adsorption measurements, the powder samples were outgases for 2 h at 200 °C.

Results and discussion

Nitrogen adsorption–desorption isotherms measured at −196 °C for MgB_2 sample are presented in Fig. 1. They are of type II according to the IUPAC classification. This type of isotherm describes the process of physical adsorption of nitrogen on the adsorbent surface. Because magnesium diboride has a heterogeneous porous structure, micro pores with the smallest diameters are filled up at low pressures of the adsorbate. With increasing adsorbate gas pressure pores of larger diameter are filled up and the multi-layer adsorption takes place. The specific surface area S_{BET} was calculated using BET method and was found equal to 6.6 $m^2\ g^{-1}$ with the corresponding total porosity varying from 0.0203 to 0.0228 $cm^3\ g^{-1}$(Table 1). The total pore volume and the pore-size distribution as presented in Fig. 2 were calculated using the Barret–Joyner–Halenda (BJH) method. The low-temperature nitrogen adsorption–desorption isotherms were used for the calculation of the fractal dimensions, based on the method presented earlier [36]. The fractal dimension characterizes the nature of adsorbents and heterogeneities of pores. This method is based on determining the sorption film surface which can

Table 1 Adsorption and porosity properties of the MgB_2 sample determined from the nitrogen adsorption–desorption isotherms

Sample	Specific surface area $S_{BET}/m^2\ g^{-1}$	Total pore volume $V/cm^3\ g^{-1}$		Adsorption value for monolayer $a_m/mmol\ g^{-1}$	Pore diameter D/nm	C_{BET}
		Ads.	Des.			
MgB_2	6.6	0.0203	0.0228	1.53	11.7	21.7

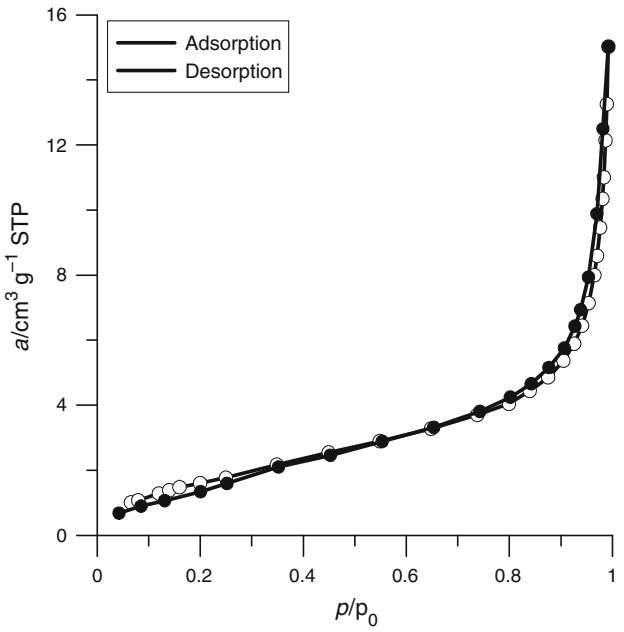

Fig. 1 Nitrogen adsorption–desorption isotherms for MgB_2 sample

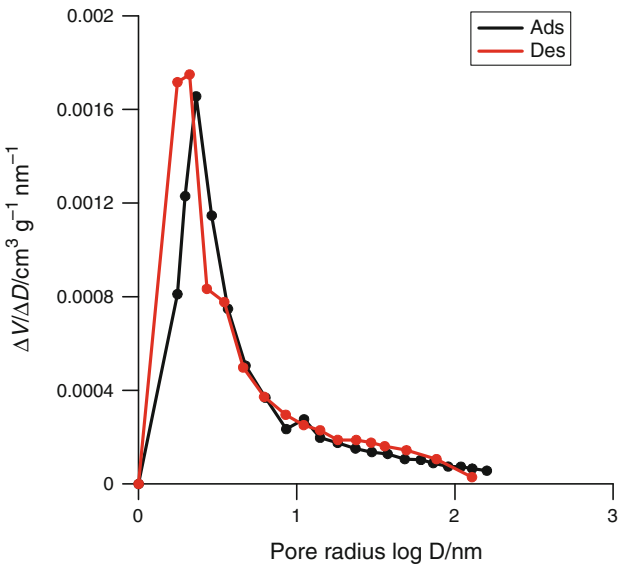

Fig. 2 Distribution functions of pore volume in relation to their radius for MgB_2 sample

Table 2 Fractal dimension values and surface roughness parameters of the MgB_2 sample determined from sorptometry and AFM data

Sample	D_f sorptometry	D_f AFM	S_a/nm	S_{ku}
MgB_2	2.49	2.88	19.2	3.75

be calculated from the Frenkel–Halsey–Hill theory and the Kiselev equation [37]. The fractal dimension D_f can be calculated from the relationships [38]:

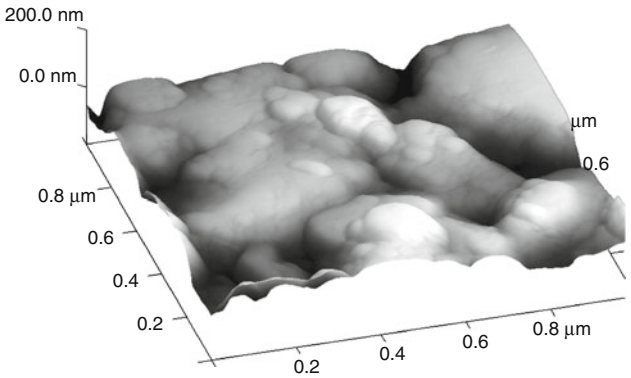

Fig. 3 AFM photograph of the surface MgB_2 sample

$$D_f = 3 - d[\ln a(x)]/d[\ln(-\ln x)] \quad (1)$$

$$D_f = 2 + d[\ln \int (-\ln x) da/d[\ln(-\ln x)] \quad (2)$$

where a is the adsorption value and x is the relative pressure.

From the obtained data, the values of the fractal dimensions were calculated using Eqs. 1 and 2. The average value and data obtained from AFM techniques are presented in Table 2. The fractal dimension (D_f) of MgB_2 increases from 2.49 (sorptometry data) to 2.88 (AFM data). Figure 3 presents AFM image of the surface MgB_2 sample. The AFM photograph scanned an area of 1000 × 1000 nm. The surface of MgB_2 is heterogeneous with the roughness average (S_a) equal to 19.2 nm (Table 2).

The fractal dimension was calculated on the basis of Fourier transformation from AFM images using commercial software Scanning Probe Image Processor (SPIP).

The fractal dimension D_f AFM is calculated for the different angles by analyzing the Fourier amplitude spectrum, for different angles the Fourier profile is extracted and the logarithm of the frequency and amplitude coordinates calculated. The fractal dimension for each direction is then calculated as 2.0 minus the slope of the log–log curves. The fractal dimension can also be evaluated from 2D Fourier spectra by application of the log log function. If the surface is fractal, the log log graph should be highly linear, with negative slope. The roughness average (S_a) and the surface kurtosis (S_{ku}) were determined from the dependences:

$$S_a = 1/MN\ \Sigma\Sigma|z(x_k, y_l) - \mu| \quad (3)$$

$$S_{ku} = 1/MNS_q^4 \Sigma\Sigma[z(x_k, y_l) - \mu]^4 \quad (4)$$

where S_{ku} describes the peak-less of the surface topography, for Gaussian height distribution S_{ku} approach 3.0 when increasing the number of pixels. Smaller values indicate broader height distribution and vice versa for values greater than 3.0, μ is the mean height

$$\mu = 1/\mathrm{MN}\,\Sigma\Sigma\,\mathrm{z}(x_\mathrm{k}, y_\mathrm{l}) \quad (5)$$

z is the local height, and MN is the analyzed area of the surface. S_q the root mean square is defined as:

$$S_\mathrm{q} = (1/\mathrm{MN}\,\Sigma\Sigma[z(x_\mathrm{k}, y_\mathrm{l}) - \mu]^2)^{1/2}. \quad (6)$$

Conclusions

Application of sorptometry and AFM techniques for the investigation of adsorbed layers and porosity parameters used for the quantitative characterization of the geometrical (e.g., total) heterogeneities of magnesium diboride are discussed. The described method is very useful to investigate physico-chemical properties of surface films, adsorbate–adsorbent interactions, and total magnesium diboride surface heterogeneity. Studies of low-temperature adsorption confirmed that the values of specific surface area (S_BET) and total pore volume depend on grain size of magnesium diboride. Comparison of sorptometry and AFM data provide new information about the adsorption and structure of the magnesium diboride. The fractal dimensions by sorptometry and AFM were 2.49 and 2.88, respectively, and they are close to each other. The difference between fractal dimensions evaluated by both methods results from the fact that the sorptometry method determined average fractal dimension of the powder sample whereas the AFM method analyzed selected surface area of the sample only.

References

1. Nagamatsu J, Nakagawa N, Muranaka T, Zenitani Y, Akimitsu J. Superconductivity at 39 K in magnesium diboride. Nature. 2001;410:63–4.
2. Rajput S, Chaudhary S. On the superconductivity and Mg outdiffusion in vacuum-synthesized MgB_2 samples. IEEE Trans Appl Supercond. 2010;20:2390–6.
3. Zhang YB, Zheng M, Gao ZS, Liu J, Zhu HM, Zhou SP. Synthesis and characterization of MgB_2-MgO composite superconductor. J Supercond Nov Magn. 2009;22:729–32.
4. Nakane T, Kumakura H. Evaluation of effect of area factors on the grain connectivity of *ex-situ* MgB_2 cores. IEEE Trans Appl Supercond. 2009;19:2793–6.
5. Braccini V, Wardelli D, Penco R, Grasso G. Development of *ex situ* processed MgB_2 wires and their applications to magnets. Physica C. 2007;456:209–17.
6. Abrahamsen AB, Grivel JC, Andersen NH, Homeyer J, Saksl K. Kinetics of MgB_2 formation studied in situ synchrotron X-ray powder diffraction. IEEE Trans Appl Supercond. 2007;17:2757–60.
7. Nakane T, Fujii H, Masumoto A, Kitaguchi H, Kumakara H. The improvement of in situ powder in tube MgB_2 tapes by mixing MgB_2 to the starting powder MgH_2 and B. Physica C. 2005;426:1238–43.
8. Bohnestiehl S, Dregia SA, Sumpton MD, Collings EW. Thermal analysis of MgB_2 formation. IEEE Trans Appl Supercond. 2007;17:2754–6.
9. Kuwashima H, Murase S, Nanato N, Kim SB, Yamada Y, Nitta A, Tachikawa K. J_c anisotropy and pinning behaviours of the in situ MgB_2 wires with/without SiC addition. IEEE Trans Appl Supercond. 2008;18:1212–5.
10. Haesler W, Rodig C, Fischer C, Holzapfel B, Perner O, Eckert J, Nenkov K, Fuchs G. Low temperature preparation of MgB_2 tapes using mechanically alloyed powder. Supercond Sci Technol. 2003;16:281–4.
11. Fischer C, Hassler W, Rodig C, Perner O, Behr G, Schubert M, Nenkov K, Eckert J, Holzapfel B, Schultz L. Critical current densities of superconducting MgB_2 tapes prepared on the base of mechanically alloyed precursors. Physica C. 2004;406:121–30.
12. Saglietti L, Perini E, Ripamonti G, Bassani E, Carcano G, Giunchi G. Boron purity effects on structural properties of MgB_2 obtained by Mg-reactive liquid infiltration. IEEE Trans Appl Supercond. 2009;19:2739–43.
13. Agostino A, Bonometti E, Volpe P, Trucatto M, Manfredoti C, Olivero P, Paolini C, Rinaudo G, Gozzelino L. Carbon influence in the synthesis of MgB_2 by a microwave methods. Int J Mod Phys B. 2003;17:773–8.
14. Paranthaman M, Thompson JR, Christen DK. Effect of carbon-doping in bulk superconducting MgB_2 samples. Physica C. 2001;355:1–5.
15. Ribeiro RA, Budko SL, Petrovic C, Canfield PC. Carbon doping of superconducting magnesium diboride. Physica C. 2003;384:227–36.
16. Lee S, Masui T, Yamamoto A, Uchiyama H, Tajima S. Carbon-substituted MgB_2 single crystals. Physica C. 2003;397:7–13.
17. Kazakov SM, Puzniak R, Rogacki K, Mironov AV, Zhigadlo ND, Jun S, Soltman Ch, Batlogg B, Karpinski J. Carbon substitution in MgB_2 single crystals: structural and superconducting properties. Phys Rev B. 2005;71:024533–024543.
18. Yuan GQ, Xu XN, Wang ZH, Lu DW, Jin X. Comparison of physical properties for carbon nanotube doped MgB_2 superconductors synthesized with different process. Physica C. 2005;432:257–62.
19. Wilke RHI, Budko SL, Canfield PC, Finnemore DK, Hannaks ST. Synthesis of $Mg(B_{1-x}C_x)_2$ powders. Physica C. 2005;432:193–205.
20. Wang JL, Zeng R, Kim JH, Lu L, Dou SX. Effects of C substitution on the pinning mechanism of MgB_2. Phys Rev B. 2008;77:174501–7.
21. Feng Y, Zhao Y, Sun YP, Liu FC, Fu BQ, Zhou L, Chen CH, Koshizuka N, Murakami M. Improvement of critical current density in MgB_2 superconductors by Zr doping at ambient pressure. Appl Phys Lett. 2001;79:3983–5.
22. Xu XL, Guo JD, Wang YZ, Wang X. Au doping effects in the $Mg_{1-x}Au_xB_2$ series. Mater Lett. 2003;58:142–5.
23. Slusky JS, Rogado N, Regan KA, Hayward MA, et al. Loss of superconductivity with the addition of Al to MgB_2 and structural transition in $Mg_{1-x}Al_xB_2$. Nature. 2001;410:343–5.
24. Gu D, Cai W, Yan YM, Cui JK, Wu YG, Yuan T, Shen GQ, Jin LJ. Effect of Pb substitution in bulk superconducting MgB_2. Physica C. 2003;386:643–7.
25. Shekhar C, Giri R, Tiwari RS, Rana DS, Malik SK, Srivastava ON. Effect of La doping on microstructure and critical current density of MgB_2. Supercond Sci Technol. 2005;18:1210–4.
26. Zhang Y, Lu Ch, Zhou SH, Chung K, Li WX. Optimization of nominal mixing ratio of Mg to B in fabrication of magnesium diboride bulk. IEEE Trans Appl Supercond. 2009;19:2775–9.
27. Williamsen GK, Hall WH. X-ray line broadening from filed aluminium and wolfram. Acta Metall. 1953;1:22–31.
28. Avdeev M, Jorgensen JD, Ribeiro RA, Budko SL, Canfield PC. Crystal chemistry of carbon-substituted MgB_2. Physica C. 2003;387:301–6.
29. Perner O, Haer W, Eckert J, Fischer C, Mickel C, Fuchs G, Holzapfel B, Schultz L. Effects of oxide addition on

superconductivity in nanocrystalline MgB_2 bulk samples. Physica C. 2005;432:15–24.
30. Serquis A, Zhu YT, Peterson EJ, Coulter JY, Peterson DE, Mueller FM. Effect of lattice strain and defects on the superconductivity of MgB_2. Appl Phys Lett. 2001;79:4399–401.
31. Kim JH, Don SX, Shi DQ, Rindfleisch M, Tomsic M. Study of MgO formation and structural defects in in situ processed MgB_2/Fe wires. Supercond Sci Technol. 2007;20:1026–31.
32. Kario A, Hassler W, Herrmann M, Rodig C, Scheiter J, Holzapfel B, Schultz L, Slachter S, Ringsdorf B, Goldacker W, Morawski A. Properties of MgB_2 tapes prepared by using MA in *ex-situ* powder. IEEE Trans Appl Supercond. 2010;20:1521–3.
33. Hanafusa K, Yamamoto A, Ogino H, Hori S, Shimoyama J, Kishio K. Interpretation of X-ray line profile of polycrystalline MgB_2. IEEE Trans Appl Supercond. 2009;19:2690–3.
34. Gallitto AA, Bonsignore G, Giunchi G, Vigni ML. Effects of weak links in the nonlinear microwave response of MgB_2 superconductor. J Supercond Nov Magn. 2007;20:13–20.
35. Tajima T, Canabal A, Zhao Y, Romanenko A, Moeckly BH, Nantista ChD, Tantawi S, Phillips L, Iwashita Y, Campisi IE. MgB_2 for application to RF cavities for accelerators. IEEE Trans Appl Supercond. 2007;17:1330–3.
36. Staszczuk P, Sternik D, Chądzyński GW, Kutarov VV. Characterization of physicochemical properties of high-temperature superconductor surfaces using nitrogen adsorption. J Alloys Comp. 2004;367:277–82.
37. Staszczuk P, Sternik D, Chądzyński GW, Robens E, Błachnio M. Studies of heterogeneity properties of selected high-temperature superconductor surfaces. J Therm Anal Calorim. 2006;86:133–6.
38. Chądzyński GW, Staszczuk P, Sternik D, Błachnio M. Studies physico-chemical properties and fractal dimensions of selected high-temperature superconductor surfaces. J Therm Anal Calorim. 2008;94:623–6.